Effects of the position of silver nanoprisms on the performance of organic solar cells*

ZHANG Qiang (张强)[1,2], **QIN Wen-jing** (秦文静)[1,2], **CAO Huan-qi** (曹焕奇)[1,2], **YANG Li-ying** (杨利营)[1,2], **ZHANG Feng-ling** (张凤玲)[1,3], **and YIN Shou-gen** (印寿根)[1,2]**

1. *Key Laboratory of Display Material and Photoelectric Devices, Ministry of Education of China, Tianjin University of Technology, Tianjin 300384, China*
2. *Key Laboratory of Display Material and Photoelectric Devices of the City of Tianjin, Tianjin University of Technology, Tianjin 300384, China*
3. *Biomolecular and Organic Electronics, Center of Organic Electronics, Department of Physics, Chemistry and Biology (IFM), Linköping University, Linköping SE-581 83, Sweden*

(Received 9 March 2014; Revised 15 April 2014)

Silver nanoprisms (AgNPs) affect the performance of organic solar cells (OSCs) in different ways depending on their positions in the device. To investigate this issue, we incorporate AgNPs in different positions of OSCs and compare their performance. The power conversion efficiency (PCE) is improved by 23.60% to 3.98% when the AgNPs are incorporated in front of the active layer. On the other hand, when AgNPs are incorporated in the back of the active layer, the short-circuit current density (J_{SC}) is improved by 17.44% to 10.84 mA/cm^2. However, if AgNPs are incorporated in the active layer, both open-circuit voltage (V_{OC}) and J_{SC} are decreased. We discuss the position effect on the device performance, clarify the absorption shadow and exciton recombination caused by AgNPs, and finally indicate that the optimal position of plasmonic AgNPs is in front of the active layer.

Document code: A **Article ID:** 1673-1905(2014)04-0253-5
DOI 10.1007/s11801-014-4041-7

Organic solar cells (OSCs) are attractive due to the advantages of low cost, light weight, mechanical flexibility and suitability for large-area fabrication. However, there are still a few disadvantages in OSCs related with the organic photoactive materials. One major disadvantage is the longer optical absorption length compared with charge-carrier diffusion length[1,2]. Although increasing the thickness of the active layer can absorb more light, the power conversion efficiency usually decreases due to the short charge-carrier diffusion length[3-6]. Introducing plasmonics by incorporating metal nanostructures into organic matrix is a promising approach to solve this problem. Plasmonic structures can improve the absorption efficiency of the active layers by preferentially scattering and exciting localized surface plasmon resonance (LSPR)[7-9].

Compared with other metal plasmons, silver plasmons are easier to prepare and exhibit high absorption coefficients in a broad range of wavelengths in ultraviolet (UV), visible (VIS) and near-infrared (NIR) portions of the spectrum[3,5,8,10]. The investigations in this area have been focused on the improvement of efficiency by using different silver nanostructures in different positions of OSCs[3,8,9]. Atwater and Poleman[7] summarized that plasmonic structures can offer at least three ways for reducing the physical thickness of the photovoltaic absorber layers, while their optical thicknesses can keep constant. These three ways include the sub-wavelength scattering when AgNPs are positioned in front of the active layer, the increased effective absorption cross-section when AgNPs are mixed in the active layer, and the surface plasmon polaritons (SPPs) excitation when AgNPs are positioned at the metal/semiconductor interface. Until now, the parallel comparison among performance of devices with AgNPs at these three positions is not to be explored.

In this paper, self-assembled AgNPs are added at different positions in devices with a structure of indium tin oxide (ITO)/ poly (3, 4-ethylenedioxythiophene): poly (styrenesulfonate) (PEDOT: PSS)/ poly(3-hexylthiophene): [6, 6]-phenyl-C61 butyric acid methylester (P3HT:PCBM)/ LiF/Al. We compare the performance of devices with the following three structures: structure a with AgNPs in front of the active layer, i.e., ITO/AgNPs/PEDOT:PSS/ P3HT:PCBM/LiF/Al; structure b with AgNPs in the back of the active layer, i.e., ITO/PEDOT:PSS/P3HT:PCBM/

* This work has been supported by the National Natural Science Foundation of China (No.60676051), the Natural Science Foundation of Tianjin (No.07JCYBJC12700), and the Foundation of Key Discipline of Material Physics and Chemistry of Tianjin.
** E-mail: sgyin@tjut.edu.cn

AgNPs/LiF/Al; and structure c with AgNPs in the active layer, i.e., ITO/PEDOT:PSS/P3HT:PCBM:AgNPs/LiF/Al. Structure a can lead to an improved power conversion efficiency (PCE) of 3.98%, which is 23.60% higher than that of control device without AgNPs (3.22%), while structure b can lead to an improved short-circuit current density (J_{SC}) of 10.84 mA/cm^2, which is 17.40% higher than that of control device. The open-circuit voltage (V_{OC}) is not influenced in these two structures. On the contrary, mixing AgNPs in the active layer (structure c) causes the decrease of V_{OC}, J_{SC} and PCE.

We used a two-step technique to synthesize AgNPs. First, silver seeds were produced by mixing 5.0 mL 2.5 mol/m^3 aqueous solution of trisodium citrate, 0.25 mL 500 mg/L aqueous solution of poly(sodium styrenesulphonate) (PSSS, 1 000 kDa, Aldrich) and 0.3 mL 10 mol/m^3 freshly prepared aqueous solution of $NaBH_4$, followed by adding 5.0 mL 0.5 mol/m^3 aqueous solution of $AgNO_3$ at a rate of 2.0 mL/min with stirring. AgNPs were then produced by mixing various amounts of the seed solution with 75 μL 10 mol/m^3 aqueous ascorbic acid solution, followed by adding 3.0 mL 0.5 mol/m^3 aqueous solution of $AgNO_3$ at a rate of 1.0 mL/min. The synthesized AgNPs were stabilized with 0.5 mL 25 mol/m^3 aqueous solution of trisodium citrate and diluted with distilled water. Finally, the AgNPs were centrifuged and dispersed in ethanol[11].

Fig.1(a)–(c) show the schematic diagrams of three investigated stack structures. For structure a, the AgNPs layer was spin coated at 800 r/min and vacuum-annealed at 90 °C for 5 min. Then these two steps were repeated to form 1–5 layers of AgNPs. A PEDOT:PSS layer was spin-coated onto the AgNPs, and annealed at 120 °C for 1 h. A P3HT:PCBM blending chlorobenzene solution (1:0.8) was spin-coated at 800 r/min for 10 s onto the PEDOT:PSS layer to form a 120 nm-thick active layer. Thermal annealing of the sample was carried out at 110 °C for 10 min on a hot plate in an argon-filled glove box before transferring to a vacuum deposition system. Finally, a 0.6 nm-thick LiF buffer layer and a 100 nm-thick Al electrode were thermally evaporated. The difference between structure b and structure a is that AgNPs were spin-coated onto the active layer in the former. For structure c, different amounts of AgNPs were dispersed in the active layer.

Particle size and morphology of AgNPs were characterized by transmission electron microscopy (TEM, 200 kV, JEOL JEM-2100 LaB6). Absorption spectra were recorded by using a U-V4100 spectrometer. Incident photon-to-current efficiency (IPCE) was measured by a current preamplifier at short-circuit condition under monochromatic light from a quartz-halogen lamp (CROWNTECH, INC). Current-voltage characteristics were recorded by a Keithley 2400 sourcemeter in the dark or under simulated AM1.5G (100 mW/cm^2).

Fig.1(d) shows the X-ray diffraction (XRD) pattern of AgNPs. The four diffraction peaks correspond to (111), (200), (220) and (311) crystal planes of face-centered cube. The inset of Fig.1(d) is the TEM image, which shows that the AgNPs have a uniform size distribution about 50–80 nm).

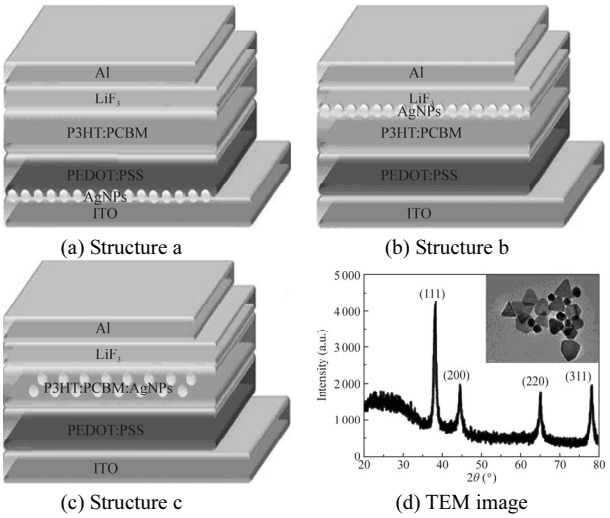

Fig.1 (a)–(c) Schematic diagrams of investigated devices with AgNPs at different positions, and (d) XRD pattern of AgNPs (The insert shows the TEM image of AgNPs.)

Fig.2(a) shows the absorption spectrum of AgNPs dispersed in ethanol. Four absorption peaks are observed at 580 nm, 400 nm, 340 nm and below 300 nm. Fig.2(b) and (c) show the UV-VIS absorption spectra of structures a and b without the electrodes, respectively. The absorption at 400–600 nm is enhanced in the two structures, and the absorption intensity is increased with the increasing layer number of AgNPs. This is likely because AgNPs can generate plasmonic scattering and enhance the absorption of the active layers. In structure a, the incident light is reflected and absorbed by the materials when it passes through the AgNP slayer and the active layer in sequence. However, the absorption shadow arises when the device contains more than 4 layers of AgNPs, and leads to a decrease in the absorption intensity. On the contrary, the absorption intensity is increased monotonically with the layer number of AgNPs located in the back of the active layer. It can be attributed to the SPP effects of the AgNPs near the back electrode.

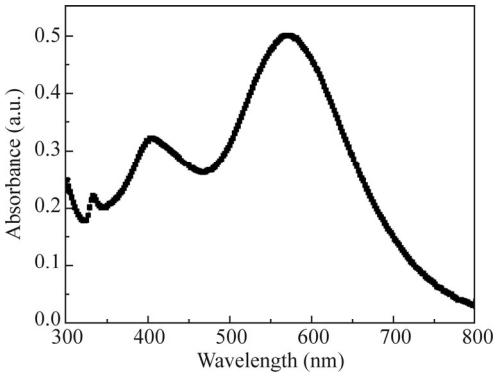

(a) AgNPs solution

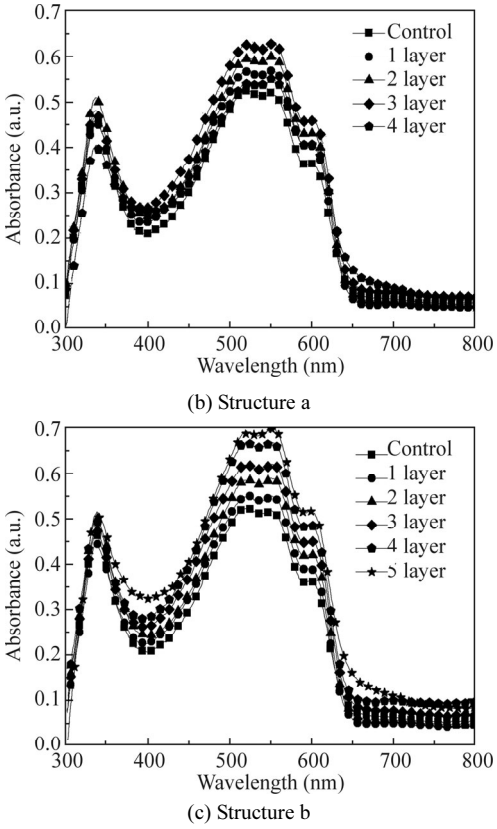

Fig.2 UV-VIS absorption spectra of AgNPs solution, structure a and structure b

We further investigate the plasmon effects of different amounts of AgNPs in structure a and structure b, and the results are shown in Fig.3. As shown in Fig.3(a), the AgNPs do not influence V_{OC} of the devices, which is mainly determined by two factors, i.e., the difference between donor's highest occupied molecular orbital (HOMO) and acceptor's lowest unoccupied molecular orbital (LUMO) and the interface contact between donor and accepter[12]. In the two structures, the introduction of AgNPs changes neither of the two factors, so V_{OC} is unchanged.

Fig.3(b) demonstrates the relationship between J_{SC} and the layer number of AgNPs in the two structures. Short-circuit current densities of both devices first increase and then decrease with the increase of the layer number of AgNPs. The increase may be attributed to the light absorption enhancement caused by the plasmon resonance scattering of AgNPs[13]. J_{SC} is decreased with further increasing the layer number of AgNPs, which is probably a result of the increased interfaces that influence the vertical transport of charges[14]. It is worth noting that structure b with 4 layers of AgNPs gives the highest J_{SC}. For structure a, the main way for increasing the light absorption is to enhance the light scattering and produce coupling electromagnetic fields. But due to the existence of absorption shadow, some incident light can not come into the solar cells, which reduces the spectral utilization in the active layer[15]. For structure b, the main way for increasing the light absorption is mostly the generation of SPPs which trap and guide the electromagnetic waves to travel horizontally in the active layer.

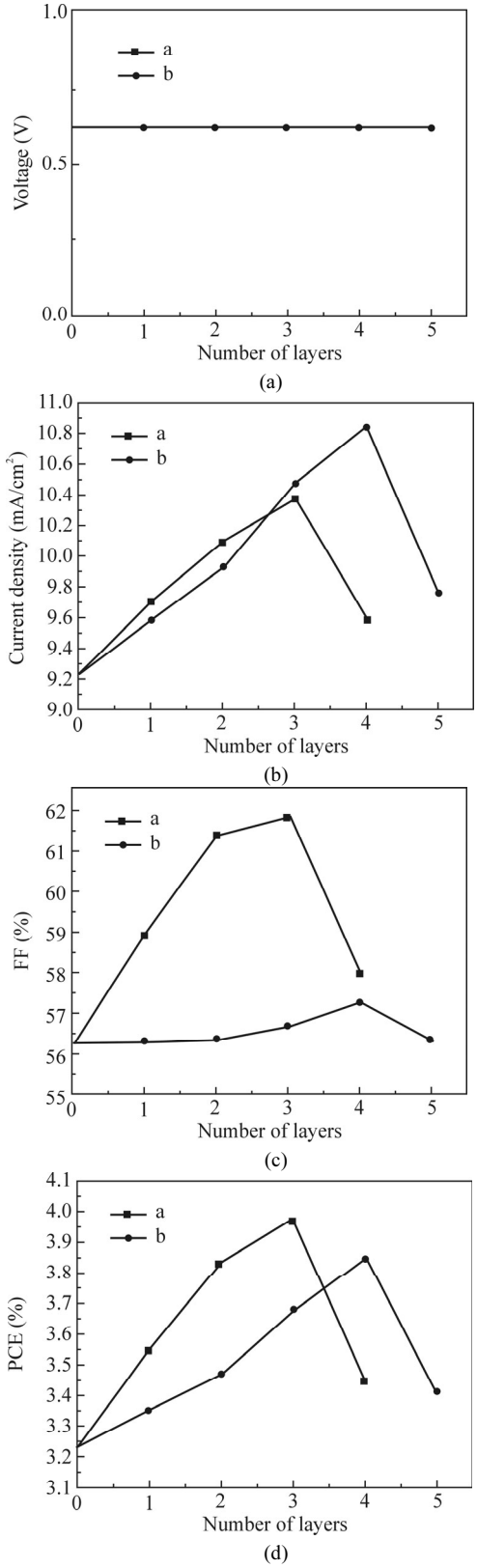

Fig.3 The comparison of (a) V_{OC}, (b) J_{SC}, (c) FF and (d) PCE of structures a and b with different layers of AgNPs

Normally, the relation between current (I) and applied voltage (V) of an illuminated photovoltaic cell follows the generalized Shockley equation as

$$I = I_0\left[\mathrm{e}^{q(V-IR_s)/nkT}-1\right]+(V-IR_s)/R_{sh}-I_L, \quad (1)$$

where I_0 is the recombination current, I_L is the light-induced electric current, n is the ideality factor, R_s is the series resistance, and R_{sh} is the parallel resistance. R_s and R_{sh} can be roughly estimated by

$$\frac{1}{R_s}\approx\left(\frac{\mathrm{d}I}{\mathrm{d}V}\right)_{I=0}, \quad (2)$$

$$\frac{1}{R_{sh}}\approx\left(\frac{\mathrm{d}I}{\mathrm{d}V}\right)_{V=0}. \quad (3)$$

Tabs.1 and 2 list the calculated values of R_sA and $R_{sh}A$, where A is the active area of the two structures with different layer numbers of AgNPs. The introduction of AgNPs in structures a and b can decrease R_sA by about 16% and 8%, and decrease $R_{sh}A$ by about 40% and 34%, respectively. The relatively large extent of decrease in resistances of structure is probably a result of reduced contact resistances between PEDOT:PSS and ITO.

Tab.1 R_sA and $R_{sh}A$ of the control device and the devices with different layer numbers of AgNPs in front of the P3HT:PCBM layer (structure a)

	R_sA (Ωcm^2)	$R_{sh}A$ (Ωcm^2)
Control	10. 62	737. 74
1 layer	9. 31	417. 36
2 layer	8. 86	385. 65
3 layer	8. 30	499. 88
4 layer	9. 15	454. 44

Tab.2 R_sA and $R_{sh}A$ of the control device and the devices with different layer numbers of AgNPs in the back of the P3HT:PCBM layer (structure b)

	R_sA (Ωcm^2)	$R_{sh}A$ (Ωcm^2)
Control	10. 62	737. 74
2 layer	8. 99	720. 98
3 layer	9. 96	353. 92
4 layer	9. 48	449. 24
5 layer	10. 59	425. 62

Fig.3(c) shows the fill factor (FF) of both structures as a function of the layer number of AgNPs. FF first increases with the increase of the layer number of AgNPs and then decreases. One possible explanation for the increase of FF is that the enhanced plasmons excited by the AgNPs generate strong electromagnetic resonance fields, promoting the exciton separation and reducing R_s[13,16,17]. Nevertheless, with further increasing the amount of AgNPs, the probability of exciton recombination is increased, which increases R_s and thereby reduces FF. Compared with structure b, AgNPs in structure a can receive more light and generate stronger electromagnetic resonance fields, thereby it promotes better separation of excitons. Hence, FFs of structure a with different layer numbers of AgNPs are significantly higher than those of structure b.

Fig.3(d) shows that the efficiencies of the devices with two different structures first increase with the increase of the layer number of AgNPs and then decrease. Although the highest J_{SC} of structure a is slightly lower than that of structure b, the comparison between the extents of increase in FF for two kinds of structures is more appreciable. As a result, the increasing slope of PCE with increasing the layer number of AgNPs is more significant in structure a than that in structure b. The best PCE of 3.98% is obtained in the device with three layers of AgNPs located between ITO and PEDOT:PSS, and it is 1.24 times of the efficiency of the control device.

Strong plasmon effects produced by AgNPs in front of the active layer can enhance the electromagnetic field around AgNPs, which increases the light absorption in the active layer and promotes the separation of excitons[13]. Therefore, PCE is increased by 23.60% with this structure. On the contrary, incorporating AgNPs in the back of the active layer can avoid the block of light and increase the optical length of incident light by SPP effect, and therefore J_{SC} is improved by 17.44%[7].

Metal nanoparticles mixed in the active layer sometimes enhance the device performance by the so-called near-field coupling effect[7,18]. To investigate whether the AgNPs also have the near-field effect, we analyze the performance of OSCs with two different concentrations of AgNPs mixed in the active layer, i.e., structure c shown in Fig.1(c). Fig.4(a) shows J-V characteristics of the devices with AgNPs and a control device without AgNPs. The introduction of high and low concentrations of AgNPs can decrease V_{OC} from 0.62 V (control device) to 0.59 V and 0.51 V, and decrease J_{SC} from 9.23 mA/cm^2 (control device) to 8.72 mA/cm^2 and 7.95 mA/cm^2, respectively. The device efficiency decreases from 3.22% (control device) to 2.47% and 1.87%, respectively. The performance decreases are likely caused by the change of the interface contact between donor and receptor. Additionally, incorporating AgNPs in the active layers increases the probability of exciton quenching, which degrades the device performance[19]. Fig.4(b) shows that mixing AgNPs in the active layer results in the decrease of IPCE. The higher concentration of AgNPs degrades IPCE more seriously than the lower one, which confirms that AgNPs act as recombination centers for excitons in the active layer, resulting in the decline of IPCE[16].

In summary, the results reported here suggest that we should think over the following three factors when considering the function of silver plasmons: (1) whether they produce absorption shadows to affect the absorption of light in the active layer or not; (2) whether they affect the carrier transport or not; (3) whether they impact the interfacial contact or not. Only when all these three factors

are considered, we can make out the effect of metal plasmons on device performance.

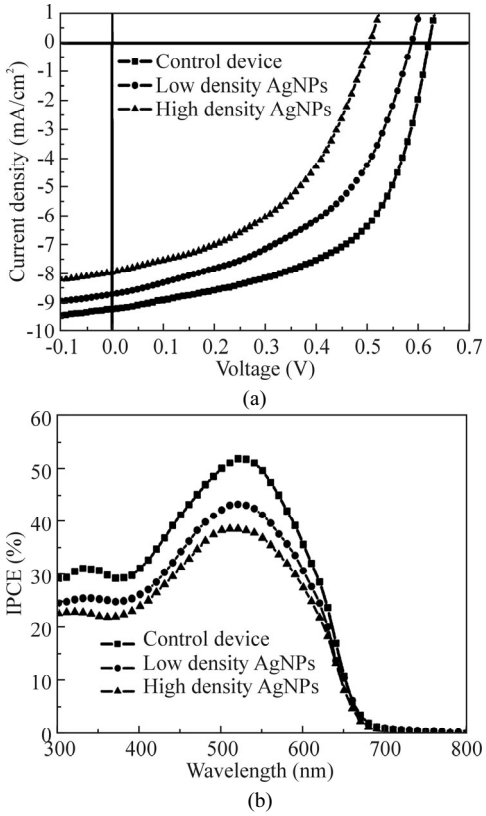

Fig.4 *J-V* and IPCE curves of control device and devices adding AgNPs with different concentrations in P3HT:PCBM

We compare the performance of photovoltaic cells with various amounts of AgNPs at three different locations. The best position of AgNPs is in front of the active layer, and PCE is improved by 23.60% to 3.98% in this case. It is higher than the PCE achieved in the structure with AgNPs in the back of the active layer, which is improved by 19.56% to 3.85%. On the contrary, AgNPs act as recombination centers when they are mixed in the active layer, and lead to exciton annihilation therein.

References

[1] LI Ming-yang, HAN Xue-song, XU Xin-rui, MA Chun-yu, YANG Li-ying, QIN Wen-jing, YIN Shou-gen and ZHANG Feng-ling, Journal of Optoelectronics·Laser **24**, 1673 (2013). (in Chinese)

[2] LI Wei-min, GUO Jin-chuan and ZHOU Bin, Journal of Optoelectronics·Laser **23**, 1274 (2012). (in Chinese)

[3] PEI Jia-ning, TAO Jin-long, ZHOU Yin-hua, DONG Qing-feng, LIU Zhao-yang, LI Zai-fang, CHEN Fei-peng and ZHANG Ji-bo, Solar Energy Materials and Solar Cells **95**, 3281 (2011).

[4] D. H. Wang, D.Y. Kim, K. W. Choi, J. H. Seo, S. H. Im, J. H. Park, O. O. Park and A. J. Heeger, Angewandte Chemie **50**, 5519 (2011).

[5] C. H. Kim, S. H. Cha, S. C. Kim, M. Song, J. Lee, W. S. Shin, S. J. Moon, J. H. Bahng, N. A. Kotov and S. H. Jin, ACS Nano **5**, 3319 (2011).

[6] QIAO Lin-Fang, WANG Dan, ZUO Li-jian, YE Yu-qian, QIAN Jun, CHEN Hong-zheng and HE Sai-ling, Applied Energy **88**, 848 (2011).

[7] H. A. Atwater and A. Polman, Nature Materials **9**, 205 (2010).

[8] H. S. Noh, E. H. Cho, H. M. Kim, Y. D. Han and J. Joo, Organic Electronics **14**, 278 (2013).

[9] LI Xuan-hua, C. W. C. Ho, LU Hai-fei, Sha Wei E. I. and A. H. Pui, Advanced Functional Materials **23**, 2728 (2013).

[10] A. P. Kulkarni, K. M. Noone, K. Munechika, S. R. Guyer and D. S. Ginger, Nano Letters **10**, 1501 (2010).

[11] D. Aherne, D. M. Ledwith, M. Gara and J. M. Kelly, Advanced Functional Materials **18**, 2005 (2008).

[12] C. M. Cardona, Wei Li, A. E. Kaifer, D. Stockdale and G. C. Bazan, Advanced Materials **23**, 2367 (2011).

[13] CHEN Fang-chun, J. L. Wu, C. L. Lee, HONG Yi, C. H. Kuo and M. H. Huang, Applied Physics Letters **95**, 013305 (2009).

[14] S. S. Kim, S. I. Na, J. Jo, D. Y. Kim and Y. C. Nah, Applied Physics Letters **93**, 073307 (2008).

[15] D. Parvathy, K. C. Wu and Z. Pei, Solar Energy Materials and Solar Cells **95**, 2102 (2011).

[16] W. J. Yoon, K. Y. Jung, Liu Ji-wen, T. Duraisamy, R. Revur, F. L. Teixeira, S. Sengupta and P. R. Berger, Solar Energy Materials and Solar Cells **94**, 128 (2010).

[17] Chuan-Dao WANG and Wallace C. H. Choy, Solar Energy Materials and Solar Cells **95**, 904 (2011).

[18] ZHANG Chun-lai, WANG Zhi-guo, LIU Chun-ming, XIANG Xia, YUAN Xiao-dong, HE Shao-bo, LI Li and ZU Xiao-tao, Acta Physica Sinica **61**, 084207 (2012).

[19] MA Chun-Yu, QIN Wen-Jing, XU Xin-rui, LI Ming-yang, HAN Xue-song, WEI Jun and YIN Shou-Gen, Solar Energy Materials and Solar Cells **109**, 227 (2013).